Proceedings of the 23rd IEEE Workshop on Control and Modeling for Power Electronics (COMPEL 2022), Tel Aviv, Israel, June 20-23, 2022

On the Size and Weight of Passive Components: Scaling Trends for High-Density Power Converter Designs

Jiarui Zou
Nathan C. Brooks
Samantha Coday
Nathan M. Ellis
R. C. N. Pilawa-Podgurski

On the Size and Weight of Passive Components: Scaling Trends for High-Density Power Converter Designs

Jiarui Zou, Nathan C. Brooks, Samantha Coday, Nathan M. Ellis, and Robert C.N. Pilawa-Podgurski
Department of Electrical Engineering and Computer Sciences
University of California, Berkeley
Email: {jiarui.zou, nathanbrooks, scoday, nathanmilesellis, pilawa}@berkeley.edu

***Abstract*—With increasing calls of electrification for transportation (e.g., electric vehicles, hybrid or electric aircraft), the need for systematic guidelines that gauge passive component specific energy density for weight-optimized converter design has become apparent. Observing a lack of data sets and corresponding modeling process for passive components that usually dominate a converter's weight, this work proposes a transformation that estimates the specific energy density of passive components from comprehensively surveyed volumetric energy density data and empirical specific density models, and thus forms a convenient guideline for converter weight optimization. The proposed model is then applied to a converter designed for electric aircraft applications to showcase the component mass estimation and selection process along with estimation accuracy.**

I. Introduction

In 2019, the transportation sector contributed to 29% of total greenhouse gas emissions within the United States [1]. As such, electric aircraft and vehicles offer appealing solutions to reduce emissions and meet renewable energy targets [2]. Enabling hybrid and fully electric vehicles requires innovations within the electric powertrain [3]. Flying capacitor multilevel (FCML) converters have shown promise for increasing performance of electric powertrains, offering light-weight and efficient solutions for dc-dc converters [4], [5] and inverters [6], [7]. One of the reasons that the FCML converter can be designed to be extremely lightweight is the use of capacitors as the primary energy storage element, which have higher energy density compared to inductors. Moreover, the FCML converter decreases the volt-second requirement on the inductor by an order of $\frac{1}{(N-1)^2}$, where N is the number of discrete levels in the switch node waveform, and thus the weight of the inductor is significantly reduced.

Accurate mass and volume information for passive components is vital for informing topology selection and optimization of lightweight converters, as passive components often dominate the weight and volume of the converter.

Fig. 1 presents the volumetric energy density trends observed as part of a comprehensive component survey, illustrating that the information associated with volume is readily accessible. However, due to the lack of mass specifications on component datasheets and distributor websites, performing weight-optimized power converter designs is more difficult for designers.

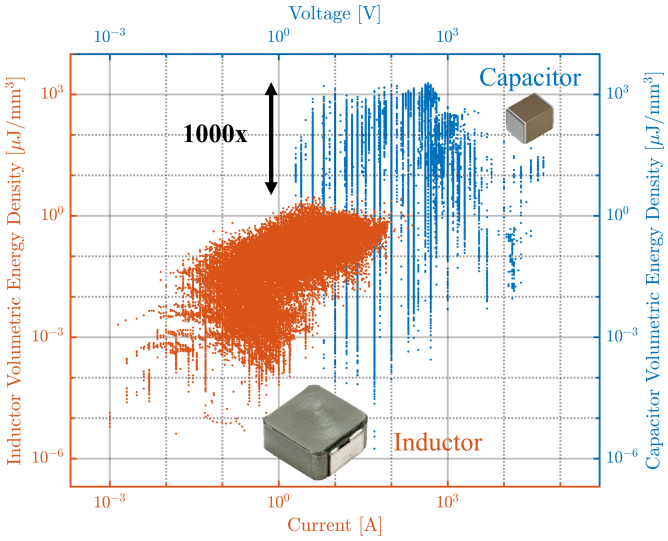

Fig. 1: A comprehensive survey (over 500,000 commercially available components) comparing the volumetric energy density of capacitors versus inductors. Up to a 1,000× difference in the fundamental energy storage capability is observed.

An FCML converter is considered in this work due to the topology's high performance in weight sensitive applications and the challenging optimization that designers face when sizing the inductive and capacitive elements. Fig. 2 shows a high-performance weight-optimized 10-level FCML converter designed for electric aircraft applications [4], [8]. The converter utilizes Class 2 multilayer ceramic capacitors (MLCCs) due to their high volumetric energy density. Since the capacitance of Class 2 MLCCs derates as the dc bias voltage across the capacitor increases, all energy density calculations of Class 2 MLCCs discussed in the paper account for the derating effect. As seen in Fig. 2b, the MLCCs contribute to 30% of the converter volume but 53% of the converter weight. Similarly, the inductor contributes only 10% of the volume, but 15% of the total weight. If different capacitor technologies (e.g., aluminum electrolytic, film, Class 1 ceramic) and inductor technologies (e.g., ferrite, air core) are implemented, the converter mass and volume breakdown could differ greatly, and thus could be optimal in volume but not in weight. This example highlights the contrast between a volume and weight-

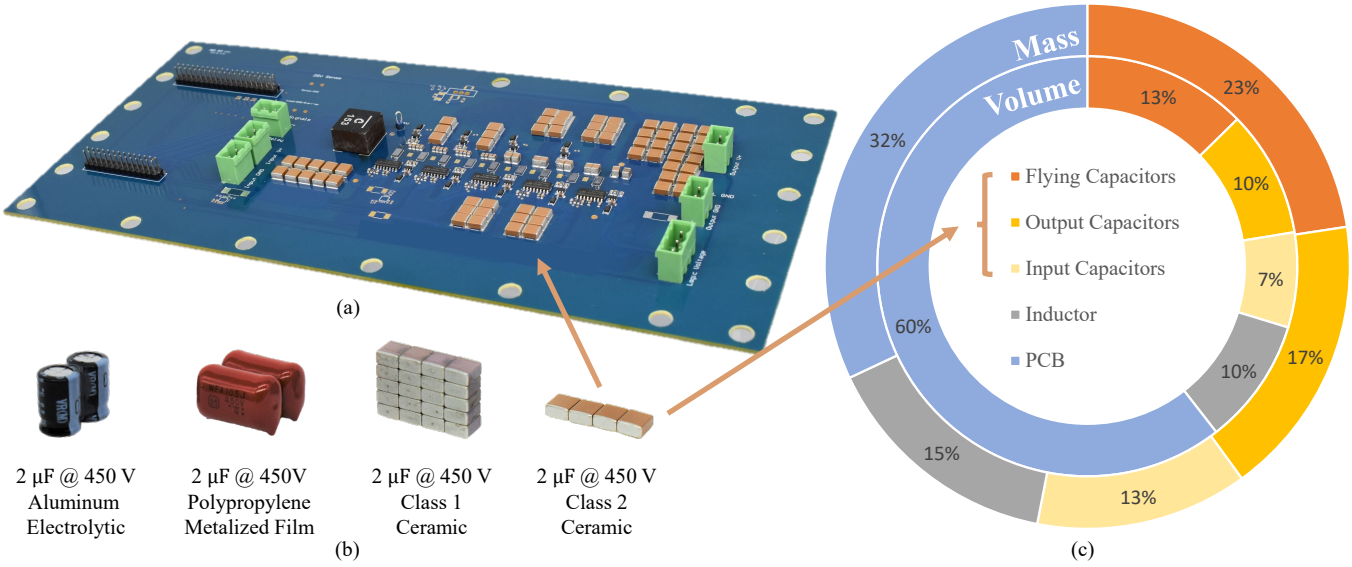

Fig. 2: (a) A high-performance 10-level FCML converter designed for electric aircraft [4]. (b) The mass and volume breakdown of the converter implemented using Class 2 multilayer ceramic capacitors. (c) Example capacitor technologies investigated in this work, showing the comparative size for the same capacitance and voltage ratings.

optimized design and indicates the need for further weight metrics.

This work proposes an empirical model for estimating a component's mass from its volume based on its technology (ceramic, aluminum electrolytic, etc.), rated voltage, and nominal capacitance. Furthermore, the modeled specific density (D = mass/volume) is applied to transform larger data sets of known volumetric energy density to estimated specific energy density. Understanding general trends in the quantified specific energy density of capacitor/inductor technologies can aid designers and further enable ultra-lightweight converter designs.

The remainder of this work will detail a method for approximating component mass and specific energy density based on known component volume and derived volumetric energy density from datasheet. Section II introduces the proposed method, Section III discusses the measurement process to obtain a large amount of component mass data with high accuracy, and Section IV provides a detailed analysis of various component mass estimation methods. Finally, Section V presents the result of specific energy density for the discussed capacitor technologies, and discusses an application example of the capacitor selection process implemented on the 10-level FCML converter shown in Fig. 2a.

II. Theory

Fig. 1 shows the result of a comprehensive survey of passive component volumetric energy density conducted by retrieving and parsing data of over $500,000$ unique commercially available components from major distributors. The volumetric energy density (γ_v) for each passive component is calculated using

$$\gamma_v = \frac{\text{Energy Stored at Rated Voltage}}{\text{Capacitor Volume}} \tag{1}$$

for capacitors and

$$\gamma_v = \frac{\text{Energy Stored at Rated Current}}{\text{Inductor Volume}} \tag{2}$$

for inductors.

As a whole, the peak volumetric energy density of capacitors (γ_v) is nearly 1,000 times higher than that of inductors. For volume-sensitive application, choosing a topology that heavily utilizes capacitors as energy transfer elements can result in a more volume efficient design [9].

Calculating volumetric energy density (γ_v) for a passive component is relatively easy since a component's package volume is typically reported on its data sheet. However,

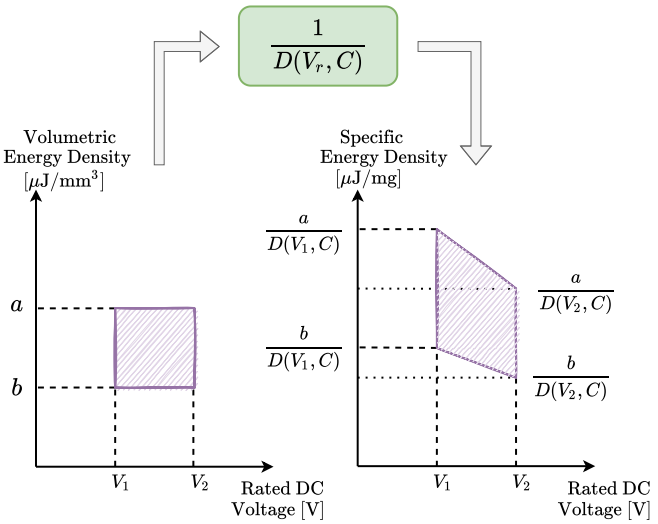

Fig. 3: Transformation of capacitor volumetric energy density to specific energy density using rated dc voltage dependent and capacitance dependent specific density.

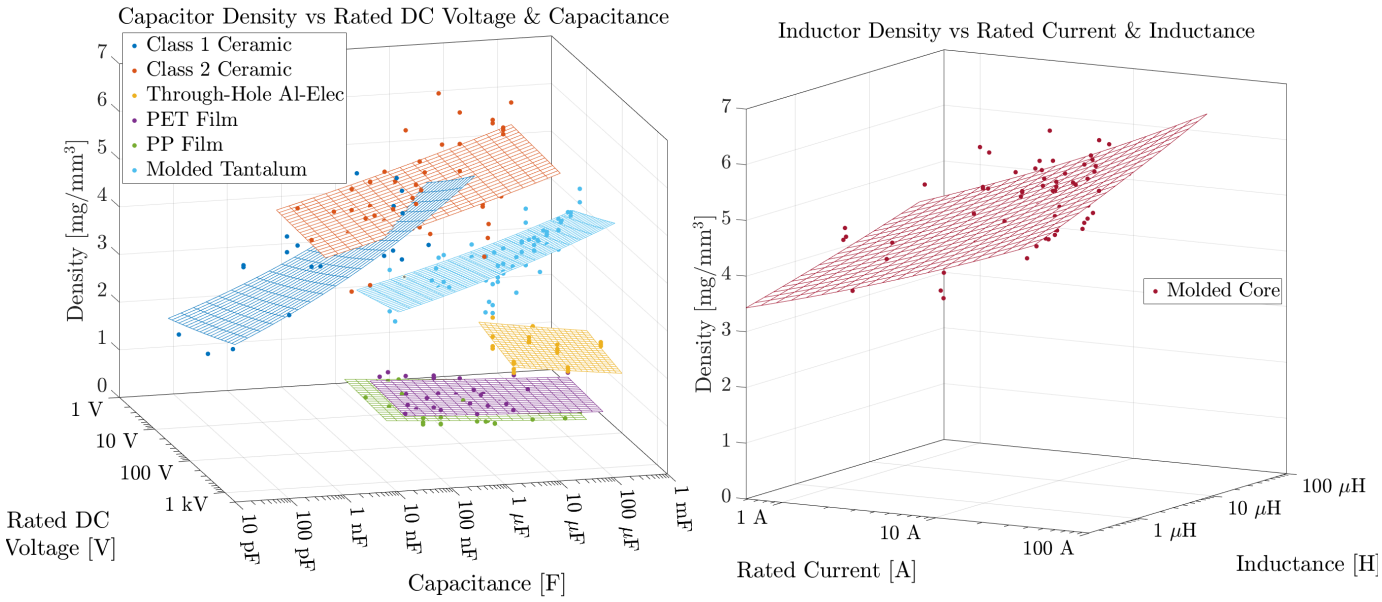

(a) (b)

Fig. 4: Empirical specific density power fits of (a) Class 1 and 2 ceramic capacitors, through-hole aluminum electrolytic capacitors, PET film capacitors, PP film capacitors, molded tantalum capacitors, and of (b) molded core inductors.

deriving the specific energy density (γ_m) is inconvenient due to the lack of consistent and accurate mass information for passive components.

A methodical transformation converting a passive component's volumetric energy density (γ_v) to specific energy density (γ_m) is proposed in this work. The component's volume is correlated to mass using its specific density D. The proposed transformation for capacitors is shown in Fig. 3 with a transformation function of $\frac{1}{D}$ since

$$\gamma_\mathrm{m} = \frac{1}{D}\,\gamma_\mathrm{v}. \tag{3}$$

III. Measurement

In total, 322 unique capacitors and 112 unique inductors were measured. For each component, multiple samples were weighed based on the accuracy of the electronic scale to limit the measurement error to a maximum of 0.5%.

To spread out the distribution of component data, capacitors were selected to cover a vast range of technologies, package sizes, rated dc voltages (V_r), capacitance (C), and manufacturers, whereas molded core inductors were selected to cover various package sizes, rated current (I_r), inductance (L), and manufacturers.

Class 1 ceramic capacitors, Class 2 ceramic capacitors, through-hole aluminum electrolytic capacitors, polyethylene terephthalate (PET) film capacitors, polypropylene (PP) film capacitors, molded tantalum capacitors, and molded core inductors were analyzed due to their prevalence in power applications such as energy storage, resonant circuits, and buffering.

IV. Data Interpretation

A. Mean Fit Estimation for Capacitor Specific Density

Given that capacitors of the same classification will likely express similar specific density (D) due to their similar material composition and construction, a mean fit is first proposed for each classification of capacitor.

Table I presents the mean fit specific density (D) for capacitors, where the mean percentage error (MPE) for N elements in each set is defined as:

$$\mathrm{MPE} = \frac{1}{N}\sum_{i=1}^{N}\frac{|D_{\mathrm{measured},i} - D_{\mathrm{predicted},i}|}{D_{\mathrm{measured},i}}. \tag{4}$$

For each of the collected data sets, the MPE is calculated to be less than 20%, showing a fairly accurate fit between the measured and the mean fit results. The error can be further reduced by improving upon the mean fit model with a more accurate power fit model dependent on the rated dc voltage and capacitance.

B. Power Fit Estimation for Capacitor Specific Density with Respect to Rated DC Voltage & Capacitance

Observing from the measured data, a correlation between specific density (D) and the capacitor parameters including rated dc voltage (V_r) and capacitance (C) emerges, thus a V_r and C-dependent energy density transformation is proposed.

After analyzing various possible fitting methods, the relationship between D, V_r, and C is determined to be best modeled by an empirical power fit shown in (5) and plotted in Fig. 4a. Table I shows the fit parameters and statistics.

$$D = k \cdot V_\mathrm{r}^{\alpha} \cdot C^{\beta} \quad \left[\frac{\mathrm{mg}}{\mathrm{mm}^3}\right] \tag{5}$$

TABLE I: Results of proposed mean fit and empirical power fit for specific density (mass/volume).

	Mean Fit		Power Fit						Accuracy Improvement
Component Type	$D\left[\frac{\text{mg}}{\text{mm}^3}\right]$	**MPE**	k	α	β	p-value	R^2	**MPE**	**MPE Reduction**
Class 1 Ceramic Capacitor	4.74	**17.1%**	11.67	0.0558	0.0665	1.02e-09	0.62	**10.0%**	**41.5%**
Class 2 Ceramic Capacitor	4.99	**11.3%**	8.406	-0.0045	0.0272	1.29e-04	0.25	**8.46%**	**25.1%**
TH Al-Elec Capacitor	1.30	**16.8%**	1.296	-0.0732	-0.0434	1.60e-03	0.33	**8.22%**	**51.1%**
PET Film Capacitor	1.33	**5.37%**	1.175	-0.0212	-0.0167	1.24e-02	0.20	**5.18%**	**3.54%**
PP Film Capacitor	1.10	**8.32%**	0.934	-0.0207	-0.0250	7.57e-09	0.55	**4.18%**	**49.8%**
Molded Tantalum Capacitor	3.62	**14.2%**	4.928	0.0482	0.0498	4.40e-08	0.43	**8.49%**	**40.2%**
Molded Core Inductor	5.58	**14.5%**	7.330	0.0903	0.0464	4.83e-14	0.52	**7.71%**	**46.8%**

All statistical p-values are significantly lower than a typical significance threshold of 0.05, confirming the modeled relationship of $D(V_\text{r}, C)$ is statistically significant. A higher R^2 value of 0.62 for Class 1 ceramic capacitors represents a lower variability of the density around the fitted model, while a lower R^2 value of around 0.2 for Class 2 ceramic capacitors and PET film capacitors express a higher variability of specific density when compared to that of Class 1 ceramic capacitors.

Table I and Fig. 4a also foreshadow interesting trends regarding the construction and properties of a capacitor technology and its electrical properties (e.g., V_r and C). To assist the interpretation of Fig. 4a and corresponding values of fitting parameters presented in Table I, the specific density power fit estimation is plotted against capacitance in Fig. 5, which is a two-dimensional projection of the three-dimensional fitting result shown in Fig. 4a.

According to (5), the fitting parameter β corresponds the slope of the specific density fitting result. As can be seen from Fig. 5, fitted specific density of Class 1 ceramic capacitors, Class 2 ceramic capacitors, and molded tantalum capacitors increases as the capacitance increases, which can also be determined by their positive β value. On the other hand, fitted specific density of though-hole aluminum electrolytic capacitors, PET film capacitors, and PP film capacitors decreases as the capacitance increases, which corresponds to their negative β value. A higher absolute value of β reflects a steeper slope for the specific density fitting result, and thus, on average, the variation in capacitance has a higher effect on the specific density. Similarly, the fitting parameter α can be used to determine the average specific density with regard to rated dc voltage.

To gauge and compare the average accuracy of the specific density predicted by mean fit estimation and power fit estimation, MPE Reduction defined as

$$\text{MPE}_\text{reduction} = \frac{|\text{MPE}_\text{mean} - \text{MPE}_\text{power}|}{\text{MPE}_\text{mean}} \tag{6}$$

is calculated and presented in Table I column MPE Reduction. The power fit estimation can further reduce the prediction error compared to mean fit estimation. As a result, designers can either utilize the mean fit estimation to quickly predict the specific density, and thus the specific energy density of a capacitor, or they can use the power fit estimation to increase the accuracy by utilizing the chosen type and rating of the capacitor without much added inconvenience.

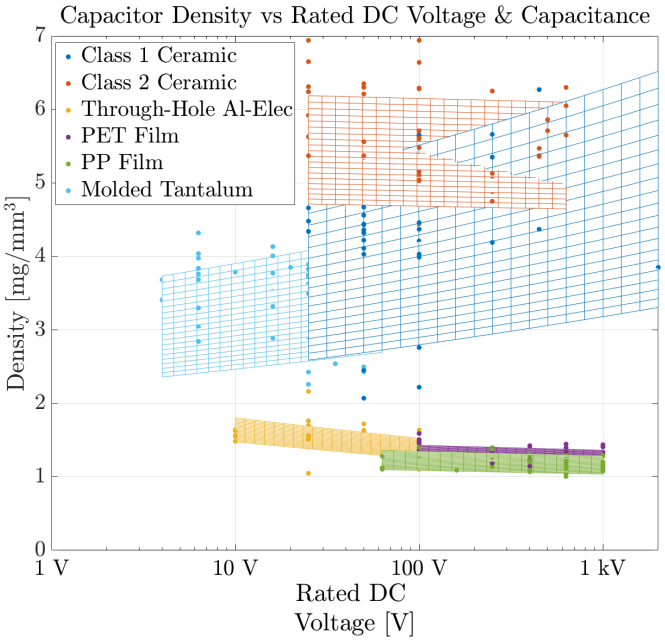

Fig. 5: Power fit estimation of specific density for the six investigated capacitor technologies plotted against rated dc voltage.

C. Power Fit Estimation for Inductor Specific Density with Regards to Rated Current & Inductance

A similar empirical fit analysis was performed with molded core inductors. Equation (7) shows the empirical power fit, and Table I and Fig. 4b show the resulting fitting model for a specific density (D) dependent on rated current (I_r) and inductance (L). As the rated current and inductance increase, the specific density of the inductor tends to increase.

$$D = k \cdot I_\text{r}^{\alpha} \cdot L^{\beta} \quad \left[\frac{\text{mg}}{\text{mm}^3}\right] \tag{7}$$

To make the model useful for practical power converters, the rated current of the inductor (I_r) was selected as the minimum of the saturation current (I_SAT) at a 20% drop of inductance and the rms current (I_RMS) at a 40 °C increase in temperature.

V. Results

A. Energy Density Transformation Result

Applying the power fit model to the transformation methodology proposed in Section II, capacitor volumetric energy density plotted against rated dc voltage shown in Fig. 6a is transformed to specific energy density shown in Fig. 6b.

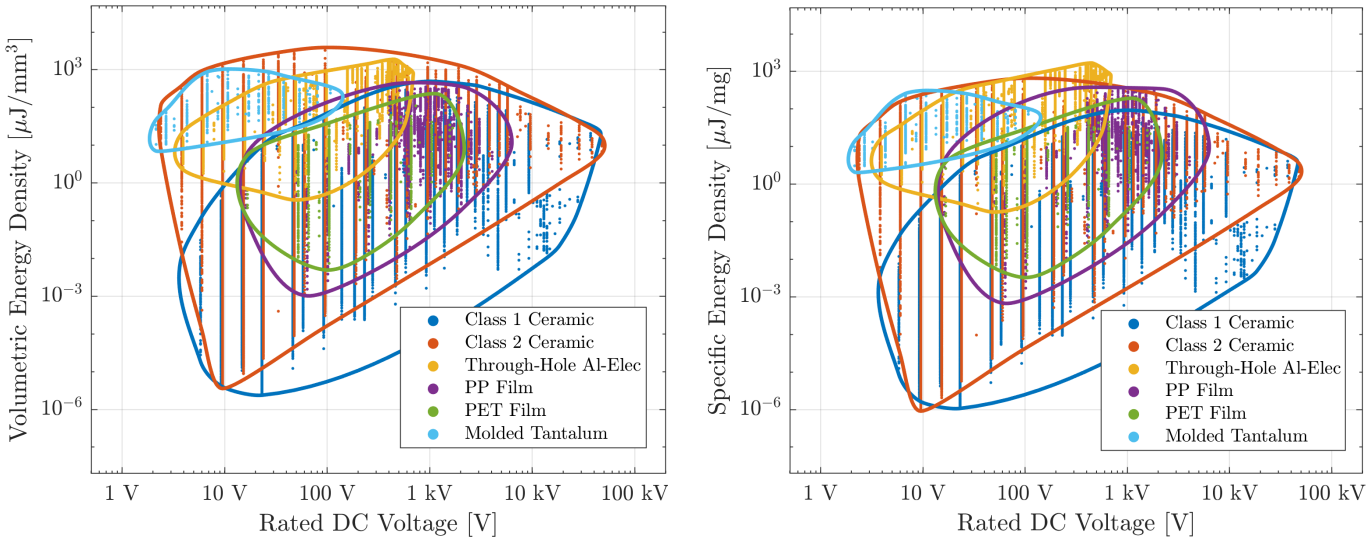

(a) (b)

Fig. 6: (a) Capacitor volumetric energy density calculated from the passive component survey. (b) Capacitor specific energy density transformed from the volumetric energy density using power-fitted specific density.

Due to the logarithmic nature of the plot and the relatively low variation of specific density within a given capacitor technology, the shape of the shaded area that encircles the energy density for a technology is similar before and after the transformation. However, the transformation reveals information about different technology's strengths and weaknesses.

The Pareto front for the energy density of each capacitor technology is defined as the curve formed by the set of capacitors that have the highest energy density at a given voltage rating. Comparing the Pareto front of the volumetric energy density for each capacitor technology in Fig. 6a, Class 2 ceramic capacitors have the highest energy density across nearly all the voltage ranges, followed closely by molded tantalum capacitors at lower voltage ranges, through-hole aluminium electrolytic capacitors at around hundreds of volts, and Class 1 ceramic capacitors and PP film capacitors at higher voltages. Hence, knowing the subtle difference between different technologies is crucial due to the close energy density competition between technologies at a given voltage rating.

After the transformation using specific density derived from power fit estimation, the position of each specific energy density is shifted slightly from that of volumetric. For specific energy density, the molded tantalum capacitors have the highest energy density at lower voltages, whereas through-hole aluminum electrolytic capacitors have significant advantage above 100 V and further increase their lead utill the technology's limit at around 700 V. PP film capacitors excel at over 1 kV and maintain their lead until around 5 kV. While previous designs have implemented class 2 MLCCs due to their high volumetric energy density, this work shows that depending on operating conditions, other capacitor technologies may actually yield even lighter weight designs when holding passive component energy storage constant.

After applying the power fit estimation to obtain the specific energy density of molded core inductors, specific energy density of all passive component technologies modeled in Section IV are plotted in Fig. 7b. Comparing to the 1,000 times difference in peak volumetric energy storage capacity shown in Fig. 7a, a even more drastic 10,000 times difference in peak specific energy storage capacity is observed, indicating the huge advantage of capacitors in lightweight converter designs.

B. Experimental Verification of the Power Fit Estimation

To verify the model presented in this work, the 10-level FCML converter presented in Fig. 2a is considered as a test bench while utilizing the information shown in Fig. 6b.

The FCML converter implements four Class 2 multilayer ceramic capacitors in parallel to create a 2 μF flying capacitor bank at the operating voltage with derating taken into consideration. At a rated voltage of 450 V, the four capacitor technologies with the highest specific energy density indicated in Fig. 6b are, from highest to lowest, aluminum electrolytic capacitors, Class 2 ceramic capacitors, PP film capacitors, and Class 1 ceramic capacitors.

Fig. 2c shows the relative volume comparison for the flying capacitor bank with equivalent capacitance at operating voltage. Using the capacitor volume calculated from provided component dimension specifications and the power fit estimation parameter provided in Table I, the specific density (D) and the total capacitor bank mass are calculated as shown in Table II.

As shown in Table II, the power fit estimation error for component mass is very low. Further more, at the same capacitance and rated voltage, aluminum electrolytic capacitors have the highest specific energy density and are indeed also the lightest. However, in addition to weight, other considerations such as ESR, suitable frequency range, rms current rating, and lifetime should be taken into account, at which point the aluminum electrolytic capacitor may not be suitable as a flying capacitor. The mass comparison of flying capacitor banks, from smallest to the largest, is in accordance with the prediction derived from Fig. 6b.

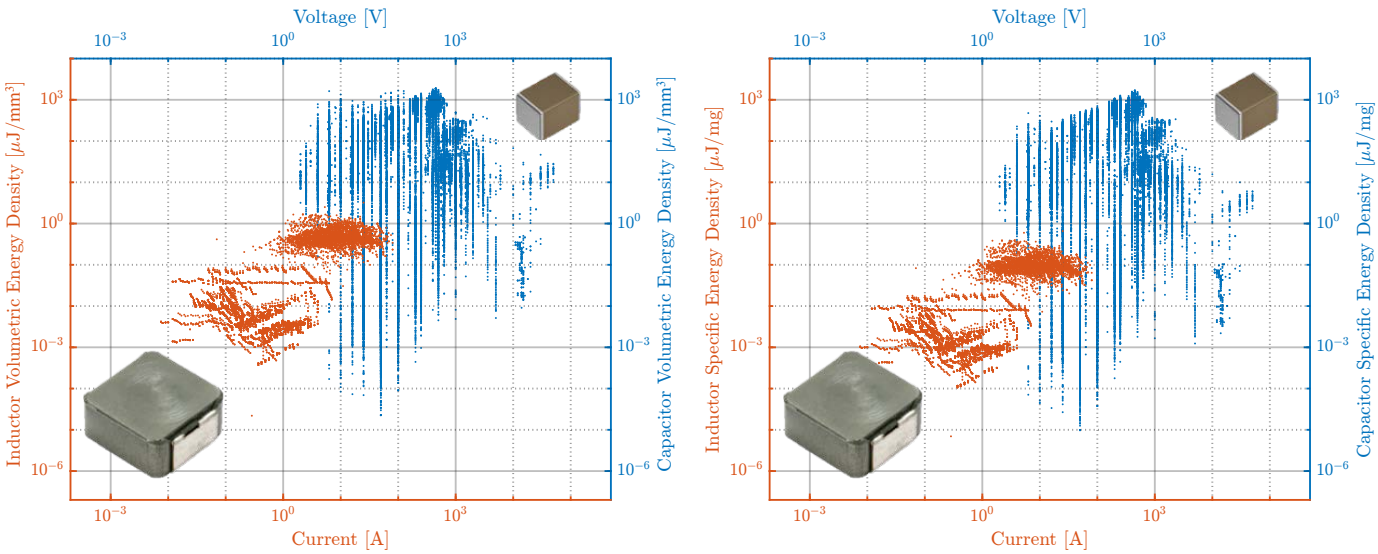

(a) (b)

Fig. 7: (a) Volumetric energy density comparison for the six investigated capacitor technologies and molded core inductor. Up to a 1,000× difference in the energy storage capability is observed. (b) Specific energy density comparison for the six investigated capacitor technologies and molded core inductor. Up to a 10,000× difference in the energy storage capability is observed.

TABLE II: Parameters for flying capacitor banks applied in the FCML converter shown in Fig. 2c including specified volume, measured and power fit estimated total mass.

	Specification	Measurement		Power Fit Estimation		Estimation Error
Component Type	Volume $\left[\text{mm}^3\right]$	$D\left[\frac{\text{mg}}{\text{mm}^3}\right]$	Mass [mg]	$D\left[\frac{\text{mg}}{\text{mm}^3}\right]$	Mass [mg]	[%]
TH Al-Elec Capacitor	810.5	1.57	1275	1.51	1223	**4.05%**
Class 2 Ceramic Capacitor	285.0	5.59	1592	5.74	1635	**2.72%**
PP Film Capacitor	3264	1.11	3626	1.16	3794	**4.65%**
Class 1 Ceramic Capacitor	1596	4.67	7452	5.62	8967	**20.3%**

While the model presented in this work can aid more accurate design of lightweight converters, expanded loss models are necessary for complete system optimizations, minimizing both loss and weight. Previous works [10], [11] have introduced a loss model for Class 2 MLCCs at low frequency large-signal excitation, and [12], [13] presented a model for high frequency dc bias dependent losses for Class 1 and Class 2 MLCCs. However, future work in analyzing and modeling operation dependent losses for a wide range of capacitor technologies is necessary to equip designers with all the information necessary for thorough design optimizations.

VI. Conclusion

This work proposes a methodology for transforming capacitor and inductor volumetric energy density to specific energy density based on estimation models of component specific density (mass/volume). Empirical mean and power fits show $< 20\%$ and $< 10\%$ errors, respectively, between the measured and modeled capacitor (and inductor) mass. Designers can use the proposed model and methodology to more systematically optimize ultra-lightweight converters.

Acknowledgement

The information, data, or work presented herein was funded in part by the Advanced Research Projects Agency-Energy (ARPA-E), U.S. Department of Energy, under Award Number DE-AR0000900 in the CIRCUITS program monitored by Dr. Isik Kizilyalli. The views and opinions of authors expressed herein do not necessarily state or reflect those of the United States Government or any agency thereof.

The information, data, or work presented herein was also funded in part by Enphase Energy.

References

[1] U.S. Environmental Protection Agency, *Sources of Greenhouse Gas Emissions*, (accessed April 1st, 2022), https://www.epa.gov/ghgemissions/sources-greenhouse-gas-emissions.

[2] P. Wheeler, T. S. Sirimanna, S. Bozhko, and K. S. Haran, "Electric/hybrid-electric aircraft propulsion systems," *Proceedings of the IEEE*, vol. 109, no. 6, pp. 1115–1127, 2021.

[3] N. M. et al, "A NASA perspective on electric propulsion technologies for commercial aviation," April 2016.

[4] S. Coday, N. Ellis, Z. Liao, and R. C. Pilawa-Podgurski, "A lightweight multilevel power converter for electric aircraft drivetrain," in *2021 IEEE Energy Conversion Congress and Exposition (ECCE)*, 2021, pp. 1507–1513.

[5] Z. Liao, Y. Lei, and R. C. N. Pilawa-Podgurski, "Analysis and design of a high power density flying-capacitor multilevel boost converter for high step-up conversion," *IEEE Transactions on Power Electronics*, vol. 34, no. 5, pp. 4087–4099, May 2019.

[6] T. Modeer, N. Pallo, T. Foulkes, C. B. Barth, and R. C. N. Pilawa-Podgurski, "Design of a GaN-based interleaved nine-level flying capacitor multilevel inverter for electric aircraft applications," *IEEE Transactions on Power Electronics*, vol. 35, no. 11, pp. 12 153–12 165, 2020.

[7] J. Azurza Anderson, G. Zulauf, P. Papamanolis, S. Hobi, S. Mirić, and J. W. Kolar, "Three levels are not enough: Scaling laws for multilevel converters in ac/dc applications," *IEEE Transactions on Power Electronics*, vol. 36, no. 4, pp. 3967–3986, 2021.

[8] S. Coday, N. Ellis, N. Stokowski, and R. C. Pilawa-Podgurski, "Design and implementation of a (flying) flying capacitor multilevel converter," in *2022 IEEE Applied Power Electronics Conference and Exposition (APEC)*, 2022, pp. 542–547.

[9] Y. Lei, C. Barth, S. Qin, W. c. Liu, I. Moon, A. Stillwell, D. Chou, T. Foulkes, Z. Ye, Z. Liao, and R. C. N. Pilawa-Podgurski, "A 2 kW, single-phase, 7-level, gan inverter with an active energy buffer achieving 216 W/in3 power density and 97.6% peak efficiency," *IEEE Transactions on Power Electronics*, vol. 32, no. 11, pp. 8570–8581, 2017.

[10] D. Menzi, D. Bortis, G. Zulauf, M. Heller, and J. W. Kolar, "Novel iGSE-C loss modeling of X7R ceramic capacitors," *IEEE Transactions on Power Electronics*, vol. 35, no. 12, pp. 13 367–13 383, 2020.

[11] D. Menzi, M. Heller, and J. W. Kolar, "iGSE-c_x – a new normalized steinmetz model for class ii multilayer ceramic capacitors," *IEEE Open Journal of Power Electronics*, vol. 2, pp. 138–144, 2021.

[12] S. Coday, C. B. Barth, and R. C. N. Pilawa-Podgurski, "Characterization and modeling of ceramic capacitor losses under large signal operating conditions," in *2018 IEEE 19th Workshop on Control and Modeling for Power Electronics (COMPEL)*, June 2018, pp. 1–8.

[13] S. Coday and R. C. N. Pilawa-Podgurski, "High accuracy calorimetric measurements and modeling of ceramic capacitor losses under large ripple operation," in *2020 IEEE Applied Power Electronics Conference and Exposition (APEC)*, 2020, pp. 188–194.